CHEMISTRY
A European Journal

A Journal of
ChemPubSoc Europe

Accepted Article

Title: Intermediates Stabilized by Tris(triazolylmethyl)amines in CuAAC Reaction

Authors: Haoqing Chen, Chengzhi Cai, Siheng Li, Yong Ma, Sijin Luozhong, and Zhiling Zhu

To be cited as: *Chem. Eur. J.* 10.1002/chem.201700555

Link to VoR: http://dx.doi.org/10.1002/chem.201700555

Supported by
ACES

WILEY-VCH

10.1002/chem.201700555

WILEY-VCH

Intermediates Stabilized by Tris(triazolylmethyl)amines in CuAAC Reaction

Haoqing Chen, [a] Chengzhi Cai,*[a] Siheng Li,[a] Yong Ma,[b] Sijin Luozhong[c] and Zhiling Zhu[a]

Abstract: Tris(triazolylmethyl)amine ligands (**TL**) are widely used to accelerate the Cu^{I}-catalyzed azide-alkyne cycloaddition (CuAAC) reaction, but its mechanistic role remains unclear. Using electrospray ionization mass spectrometry, for the first time we detected the trinuclear **TL**-Cu^{I}_3-acetylide and the dinuclear **TL**-Cu^{I}_2-acetylide complexes in aqueous solution. The apparent second-order rate constants of their reaction with an azide were 27 $M^{-1}•s^{-1}$ and 783 $M^{-1}•s^{-1}$ when the alkyne was tethered to **TL**. In the catalytic system without the tether, the rate constant increased to >146 $M^{-1}•s^{-1}$ for the **TL**-Cu^{I}_3-acetylide, but dropped by ~14 times to ~55 $M^{-1}•s^{-1}$ for the **TL**-Cu^{I}_2-acetylide. The results indicated that **TL** accelerated the reaction by stabilizing the Cu^{I}_2- and Cu^{I}_3-acetylide and their azide adduct intermediates, but this role is largely weakened by excess alkyne and other competing ligands under catalytic conditions.

Introduction

The high efficiency, orthogonality and versatility of the Cu^{I}-catalyzed azide-alkyne cycloaddition (CuAAC, a click reaction)[1] has rendered it a powerful tool in many fields.[2] The reaction was proposed to proceed through a rate-limiting transition state containing two Cu^{I}.[3] However, identification of the Cu^{I}_2-acetylide and -triazolide intermediates was hampered by the facile ligand exchange and multiple fast equilibria between the Cu^{I} complexes that are also air-sensitive and prone to aggregation and disproportionation.[4] To overcome these hurdles, strong Cu^{I} ligands, such as N-heterocyclic carbenes (NHC),[5] cyclic (alkyl) (amino) carbenes (CAAC),[6] and organophosphines[7] were employed to stabilize the Cu^{I} intermediates, allowing for isolation of single crystals of NHC-Cu^{I}-acetylide cluster,[8] (NHC-Cu^{I})$_1$-triazolide,[5a] (CAAC-Cu^{I})$_2$-acetylide and (CAAC-Cu^{I})$_2$-triazolide.[6] Also, organophosphine-stabilized Cu^{I}_2-acetylide and -triazolide intermediates were detected by electrospray ionization mass spectrometry (ESI-MS),[7] an important tool for studying the real-time distribution of reaction intermediates.[9] Using isotopically labeled Cu^{I}, Worrell *et al*. demonstrated the necessity of a second Cu^{I} atom to activate the NHC-Cu^{I}-acetylide for C-N bond formation with an organic azide.[5b]

The above progress was made using strong Cu^{I} ligands. In comparison, it is more challenging to study the mechanism of CuAAC reaction accelerated by weaker ligands, such as the tris(triazolylmethyl)amines[10] (**TL**, Scheme 1A) that are among the most efficient and widely used ligands in CuAAC reaction.[2c, 2e, 11] Although a catalytic cycle involving di-Cu^{I} acetylides formed from Cu^{I}_2**TL** was proposed (Scheme 1A),[12] the proposed intermediates were not detected. To facilitate the interception of the weakly coordinated intermediates, we tethered the **TL** with an alkyne via an EG_{11} chain as in **1** (Scheme 1B). This model system entropically stabilized the **TL**-Cu^{I}-acetylide intermediates, allowing us to evaluate their reactivity using ESI-MS.

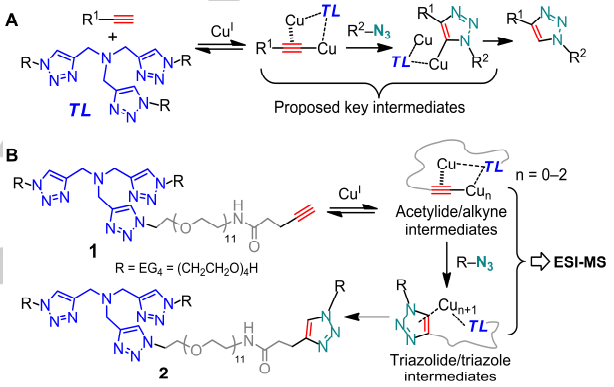

Scheme 1. (A) Previously proposed di-Cu^{I} intermediates involved in **TL**-accelerated CuAAC reaction,[12] and (B) our model system to facilitate interception of the intermediates. Charges are omitted.

Results and Discussion

We first attempted to prepare the Cu^{I}_2**TL** complex by mixing **TL** with $[Cu(MeCN)_4PF_6]$ (2 equiv.) in MeCN under N_2 followed by lyophilization to completely remove MeCN. After addition of water, the Cu/**TL** 2:1 mixture turned into a greenish-yellow suspension with red precipitates, indicating disproportionation of the free Cu^{I} into Cu^{II} and Cu^{0} (Figure S1A). In comparison, the aqueous solutions of Cu^{I}/**1** 1:1–3:1 remained colorless and clear for 4 months (Figure S1B). The ESI-MS spectra of Cu^{I}/**1** 1:1–3:1 solutions (Figure 1A) showed a mixture of Cu^{I}-alkyne and -acetylide complexes. Each major signal was assigned to a Cu^{I} complex ion based on the matches with the predicted *m/z* value and isotopic pattern (Figure S3), and their relative abundance was estimated by the ESI-MS intensities based on the evidences that indicating these Cu^{I} complex ions had a similar ESI-MS response factor (Figure S5 & Figure 1A). According to the following discussion, their structures were proposed in Scheme 2.

In the Cu/**1** 1:1 solution (Figure 1A), the predominant species was the protonated Cu^{I}-alkyne complexes (**Ia**/**Ib**). Increasing the Cu/**1** ratio to 2:1 led to a mixture of mostly **Ia**/**Ib**, the Cu^{I}_2-alkyne complex **IIa**, and the Cu^{I}_3-acetylide complex **III**a ($[\mathbf{1}–H+3Cu]^{2+}$).

[a] Prof. C. Cai, H. Chen, Dr. S. Li, Z. Zhu,
Department of Chemistry
University of Houston
3585 Cullen Blvd., Houston, Texas 77204-5003, United States
E-mail: cai@uh.edu
[b] Dr. Y. Ma
Department of Pharmacological and Pharmaceutical Sciences
University of Houston
1441 Moursund St., Houston, Texas 77030, United States
[c] S. Luozhong
Department of Chemical Engineering
Tsinghua University
Beijing, 100084, China

Supporting information for this article is given via a link at the end of the document.

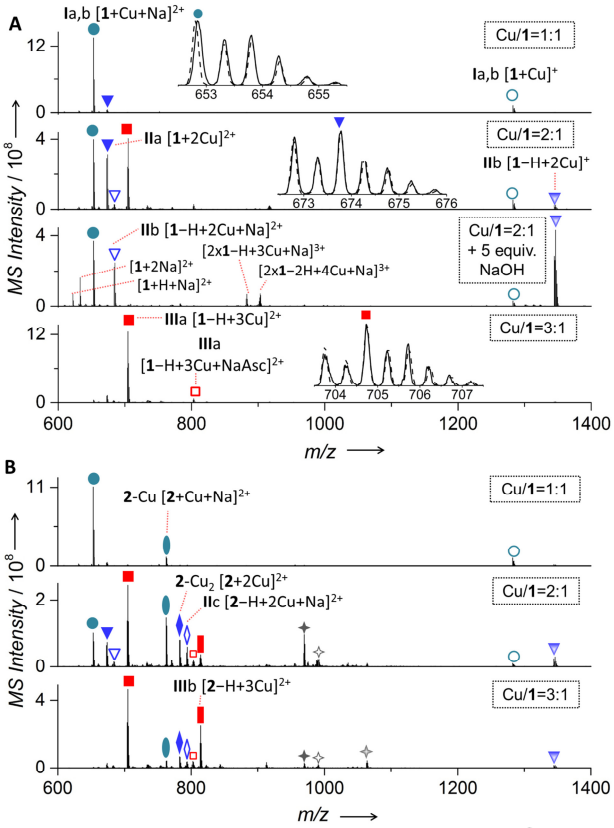

Figure 1. (A) ESI-MS spectra for solutions of **1** (100 µM) and 1–3 equiv. of Cu^{I} generated from $CuSO_4$ (100–300 µM) and Na ascorbate (1 mM) in deoxygenated water. (B) Averaged ESI-MS spectra of the above solutions (without NaOH) taken between 4–6 min after addition of 1 equiv. of N_3EG_4. All marked peaks are assigned and color-coded with cyan for mono-Cu^{I}, blue for di-Cu^{I} and red for tri-Cu^{I} species (Scheme 2). The assignment is based on a good fit of the experimental (solid lines) and theoretical (dash line) isotopic patterns (Figures S3 & S4, selected examples are shown in inserts).

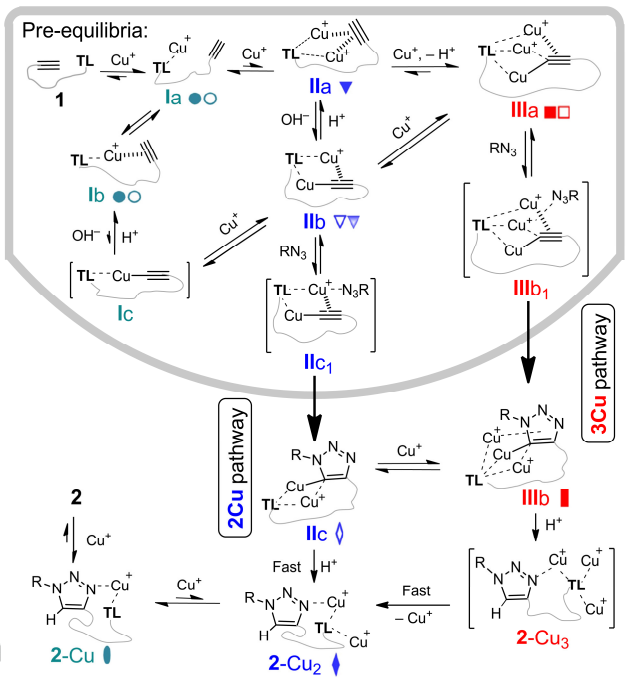

Scheme 2. Proposed mechanism for the reaction of **1** and an azide in the presence of 1–3 equiv. of Cu^{I}. Labels for the observed ions in Figures 1 & 2 are placed under the proposed mono- (**I**, cyan), di- (**II**, blue) and tri- (**III**, red) Cu^{I} complexes. The proposed intermediates in a bracket were not detectable in the ESI MS. The grey curves represent the long, flexible EG_{11} linker.

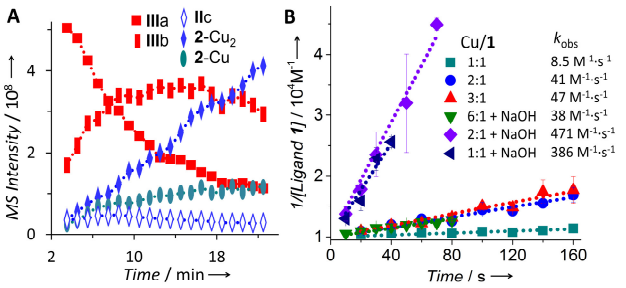

Figure 2. (A) Time course of ESI-MS intensities of the assigned intermediates during the reaction of **1** with N_3EG_4. Conditions: 100 µM **1**, 300 µM $CuSO_4$, 100 µM N_3EG_4 and 1 mM Na-Ascorbate in deoxygenated water at room temperature. For the labels, see Scheme 2. (B) Apparent second order rate constants (k_{obs}) for reaction of **1** with N_3EG_4 quantitatively measured by LC-MS. Conditions: 100 µM **1**, 100 µM N_3EG_4 and 1 mM Na-ascorbate in deoxygenated water at room temperature, with: 100 µM $CuSO_4$ (cyan); 200 µM $CuSO_4$ (blue); 300 µM $CuSO_4$ (red); 600 µM $CuSO_4$ & 500 µM NaOH (green); 200 µM $CuSO_4$ & 500 µM NaOH (purple); and 100 µM $CuSO_4$ & 500 µM NaOH (navy). Data from Figure S15.

Only ~5% of the deprotonated Cu^{I}_2-acetylide **II**b was present. At the ratio of Cu/**1** 3:1, **III**a became the predominant species (see also Table 1). Addition of NaOH produced more Cu^{I}_2-acetylide **II**b (Figures 1A, S7 and Table 1). Overall, the stability of acetylides in aqueous solution increased as the number of Cu^{I} coordination became higher (stability: **III**a > **II**b > **I**c). Indeed, **III**a was present even in the Cu/**1** 1:1 mixture at pH 6, while **I**c was not detectable (see Figure S8 for the amplified MS spectra).

The coordination mode of **III**a was proposed (Scheme 2) based on the crystal structure of a **TL**-Cu^{I}_3-acetylide analogue.[13] The interaction between Cu^{I} and alkyne or acetylide in the Cu/**1** mixtures in D_2O was evidenced by the large ^{1}H NMR downfield shift (0.19–0.58 ppm) of the propargylic protons (Figure S6).

Addition of 1 equiv. of the azide N_3EG_4 (Scheme 1B) to the solutions of Cu/**1** 1:1–3:1 generated new signals (Figure 1B) assigned to the Cu_2-triazolide **II**c and Cu_3-triazolide **III**b, and the Cu-triazole complexes **2**-Cu_2 and **2**-Cu (Scheme 2, see Figures S4 & S9–S11 for the isotopic patterns and tandem mass spectrometry analysis). Although an organophosphine-stabilized azide-Cu^{I}_2-acetylide adduct was reported,[7] the unstable adducts **II**c1 and **III**b1 in our system (Scheme 2) were not detectable.

The reactivity of the unprecedented tri-nuclear complex **III**a was first investigated by monitoring the reaction of the Cu/**1** 3:1 mixture (containing ~86% **III**a, Table 1) with 1 equiv. of N_3EG_4. As shown in Figure 2A, the MS intensity of **III**a dropped

drastically during the first 10 min, accompanied by a rapid increase of the Cu^{I}_3-triazolide **III**b whose signal intensity exceeded that of **III**a after 10 min, then decreased after ~15 min. Consumption of **III**a and accumulation of **III**b as the most abundant intermediate were faster than the formation of the triazole complexes **2**-Cu_2 and **2**-Cu, which was possibly via hydrolysis of **III**b to the transient **2**-Cu_3 followed by dissociation of Cu^{I} from **2**-Cu_3 to **2**-Cu_2, or from **III**b to **II**c followed by hydrolysis (Scheme 2).

The coordination mode of Cu_3-triazolide **III**b is tentatively proposed in Scheme 2 and Figure S14. The three coordinating Cu^{I} ions greatly stabilized **III**b against hydrolysis compared to the Cu_2-triazolide **II**c (showing a low intensity throughout the reaction, Figure S13) and the Cu-triazolide **I**c (not detectable).

We next compared the reactivity of the tri-copper acetylide **III**a with the di-copper acetylide **II**b as the key intermediate in the proposed mechanism.[3] To enrich the deprotonated **II**b, 5 equiv. NaOH was added to the solution of Cu/**1** 2:1 generating the highest percentage of **II**b (67%, Table 1) among all Cu_n-alkyne/acetylide species (Figure S7); further addition of the base promoted formation of dimers and CuOH. The stoichiometric reactions of **1** with N_3EG_4 in the presence of 1–6 equiv. of Cu^{I} (and 5 equiv. of NaOH) were quantitatively analyzed by LC-MS and their apparent second order rate constants (k_{obs}) were determined (Figures 2B, S15, and Table 1). It is generally agreed that the first C-N bond formation from the Cu_2-acetylide-azide adduct is the rate-limiting step for CuAAC reaction.[3d-f, 14] We assume that the C-N bond can be formed through the di-copper and the tri-copper pathways via the azide adducts **II**c1/**III**b1 (Scheme 2), and their barrier is much higher than those of the pre-equilibria. Under these assumptions, Eq. (1) derived from a generalized pre-equilibrium approximation method[15] and the data in Table 1 can be used to extract the apparent rate constants for converting **II**b to **II**c (k'_{II}) and **III**a to **III**b (k'_{III}):

$$k_{obs} = x_{IIb}k'_{II} + x_{IIIa}k'_{III} \qquad \text{Eq. (1)}$$

in which x_{IIb} and x_{IIIa} are the molar fraction of **II**b and **III**a derived from the ESI-MS intensities of the intermediates. Fitting the data to Eq (1) gives k'_{II} = 783 $M^{-1}•s^{-1}$ and k'_{III} = 27 $M^{-1}•s^{-1}$ (Table S1) with a good agreement between the calculated rate constants k_{cal} and the measured k_{obs} (Table 1). The ratio of k'_{II}/k'_{III} = 29:1 agreed with result of our DFT calculation showing that the barrier for C-N bond formation via a Cu_2 transition state was ~ 2 kcal/mol lower than via a Cu_3 transition state (unpubilished result).

The apparent rate constants k'_{II} and k'_{III} depend primarily on the energy barriers for the C-N bond formation, but they can also be significantly affected by any hidden equilibria interfering the transformation. These equilibria include dissociation of the azide adduct and its association with other ligands in the system, which are minimized in the model system. Specifically, the ~50 Å EG_{11} linker in **1** maintained a relatively high local concentration (in millimolar range) of the alkyne, which stabilized the **TL**-Cu_n-acetylides (**III**a/**II**b) and their azide adducts (**III**b1/**II**c1) against dissociation, and yet should not change the barrier for the C-N bond formation. In the Cu/**1** ≥ 2 system, there was no extra ligand interacting with the di- and tri-Cu acetylides and their azide adducts. Hence, the apparent rate constants k'_{II} and k'_{III} measured with this system better represents the barriers for the C-N bond formation than with a catalytic system (see below).

Table 1. MS Intensities of the Cu^{I}-acetylides in Ligand **1** System, and Observed Rate Constants (k_{obs}) vs. Calculated Rate Constants (k_{cal})[a]

Cu/**1**/NaOH[b]	ESI MS Intensity / 10^7				k_{obs} $M^{-1}S^{-1}$	k_{cal} [a] $M^{-1}S^{-1}$
	Ia/**I**b	**II**b	**III**a	**II**a		
1:1:0	149.0	1.5	0.8	5.3	9	8
2:1:0	45.1	5.4	43.7	31.6	41	43
3:1:0	4.3	4.7	132.0	12.3	47	47
1:1:5	47.2	45.9	0	0	386	386
2:1:5	40.2	67.2	0.8	0.7	471	483
6:1:5	1.2	6.3	185.0	5.0	38	50

[a] Rate constant calculated using Eq. (1), in which k'_{II} = 783 $M^{-1}s^{-1}$ and k'_{III} = 27 $M^{-1}s^{-1}$. [b] The molar ratio of added NaOH.

Overall, this model system showed a much higher k_{obs} (9–471 $M^{-1}•s^{-1}$) than the previously reported values (k_{obs} = 0.002 3.5 $M^{-1}•s^{-1}$) for CuAAC reaction accelerated by **TL** ligands (without the linked alkyne, see Scheme 1A for structure of **TL**).[12b] Compared to the above model system, reaction of the alkyne **3** and the azide N_3EG_4 under catalytic conditions (Figure 3A) showed much lower k_{obs} values of 2.1–3.6 $M^{-1}•s^{-1}$ at **3**/Cu = 10:6 (Table S2), which further decreased to 0.3–0.4 $M^{-1}•s^{-1}$ at lower catalyst loading (**3**/Cu = 100:6, Table S3).

First of all, both the di-Cu acetylide (**iia**, [**3** H+**TL**+2Cu]$^+$) and tri-Cu acetylide (**iiia**, [**3** H+**TL**+3Cu]$^{2+}$) were present under catalytic conditions (Figures 3B, S17 and S22). The ratio of [**iiia**]/[**iia**] increased with higher Cu/**TL** ratio and catalyst loading (Tables S2 and S3). Without **TL**, no di- and tri-Cu acetylide was detected (Figure S17) and the reaction was 25 times slower (Figure S20), consistent with the role of **TL** to stabilize these active species.

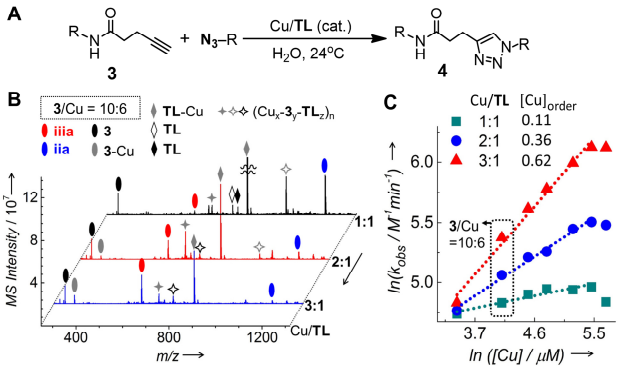

Figure 3. (A) CuAAC reaction of the alkyne **3** and RN_3 (R = EG_4). (B) ESI-MS spectra for the solutions of **3** (100 μM), **TL** (20, 30, 60 μM), Cu^{I} (60 μM) and Na-ascorbate (0.5 mM) in deoxygenated water. For assignment of the labeled ions, see Figure S18 & S19. (C) Effect of Cu^{I}/**TL** ratio on reaction order to [Cu], with **3** (100 μM), N_3EG_4 (100 μM), Cu^{I} (30, 60, 90, 120, 180, 240, 300 μM), Cu/**TL** (1:1, 2:1, 3:1). See also Table S2 for the amount of **iii**a and **ii**a vs k_{obs} at **3**/Cu = 10:6 (boxed in C, data taken from B).

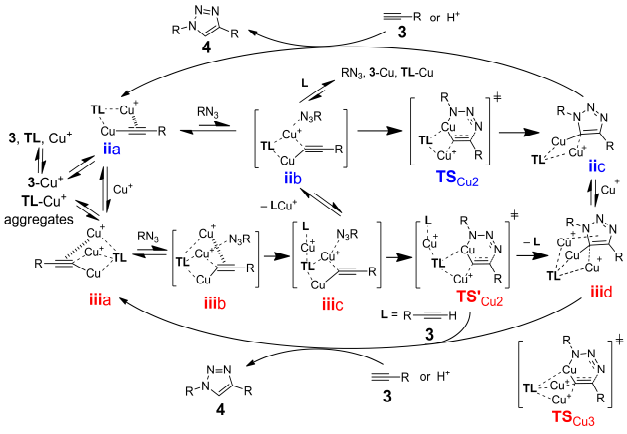

Scheme 3. Proposed mechanism for the CuAAC reaction of **3** and RN_3 (R = EG_4) in the presence of catalytic amount of Cu^I/**TL**. For the intermediates detected by ESI-MS, see Figures 3, S17-S19 and S22; intermediates in a bracket were not detectable. **L** = ligands **3** and **TL**, etc.

The slow kinetics under catalytic conditions can be attributed mainly to the dissociation of the Cu_n-acetylides **ii**a/**iii**a and their azide adducts **ii**b/**iii**b in which the Cu-acetylide bond was weakened by azide-coordination.[14] The dissociation was enhanced both by the increased entropy (compared to the EG_{11}-tethered **1** system) and by the excess alkyne and **TL** (Scheme 3), generating inactive Cu complexes **3**-Cu, **TL**-Cu, and Cu-acetylide aggregates (Figures 3 and S17). These equilibria led to fractional rate orders in [Cu] (especially at a low Cu/**TL** ratio, Figure 3C), and greatly decreased the apparent rate constant for the C-N bond formation via the di-Cu pathway (k'_{II}) by ~14 times to ~55 $M^{-1}\bullet s^{-1}$ (Tables S2 and S3).

In sharp contrast to the di-Cu pathway, the apparent rate constant for the C-N bond formation via the tri-Cu pathway (k'_{III}) was increased by 5 9 times to 146 260 $M^{-1}\bullet s^{-1}$ (Tables S2 and S3). Accordingly, the k'_{II}/k'_{III} ratio drastically dropped from 29 in the model system to <0.4 in the catalytic system (Tables S1-S3), showing a greatly enhanced contribution to k_{obs} by the tri-Cu acetylide **iii**b (for an example, see Figure 3B,C). To rationalize this result, we note that compared to the di-Cu acetylide **ii**b, the tri-Cu acetylide **iii**b has higher affinity with the negatively charged internal nitrogen of azide.[3b, 3g, h, 10f, 16] As illustrated in Scheme 3, ligand coordination to the tri-Cu-acetylide-azide adduct **iii**b will facilitate the dissociation of a Cu^I (internally) from the acetylide **iii**c to generate a di-Cu transition state $\mathbf{TS}_{Cu2}$ via **ii**b or $\mathbf{TS'}_{Cu2}$ (through the internal dissociation) for C-N bond formation. Furthermore, the triazolides **ii**c and **iii**d (detected by ESI-MS, Figure S22) may serve as a base to deprotonate the alkyne **3**, especially those formed from $\mathbf{TS'}_{Cu2}$ in which the coordinated alkyne is proximal to the triazolide, to generate the product **4** and regenerate the copper acetylides **ii**a and **iii**a (Scheme 3).

Conclusions

In summary, we reported the first example of tri-Cu-acetylide as a key intermediate in CuAAC reaction. A similar intermediate was proposed by Meldal and Tornøe.[2a] Compared to the di-Cu-acetylides, the tri-Cu-acetylide showed superior stability against protonation in aqueous solution at neutral pH. The **TL** ligand stabilizes the **TL**-Cu^I_n-acetylide (n = 2, 3) complexes and their azide adducts as the reactive intermediates, but the strength of stabilization is limited, especially at a low catalyst loading where the complexes are destabilized by the large excess of alkyne and other competing ligands.

Experimental Section

ESI-MS analysis for intermediate solution equilibria in Cu^I_n1 solutions w/ or w/o N_3EG_4 (Figure 1 & Figure 2A)

ESI-MS spectra of Cu^I_n**1** solutions and the CuAAC reaction mixtures (with N_3EG_4) were acquired using a Thermo Finnigan LCQ Deca XP Plus ion trap mass spectrometer at capillary temperature of 40°C, spray voltage 4 kV, capillary voltage 28 V, multipole 1 offset 3 V, multipole 2 offset 12 V, entrance lens voltage 61 V. In an anaerobic chamber, all stock solutions were prepared in deoxygenated Milli-Q water.

To study the solution equilibria of Cu^I_n**1** complexes (Figure 1A), 100 µL 1 mM ligand **1**, 100/200/300 µL 1 mM $CuSO_4$, 100 µL 10 mM Na ascorbate, and 700/600/500 µL deoxygenated water were mixed in 3 separate Eppendorf tubes in an anaerobic chamber, vortexed, and then directly infused into the ESI source by a syringe pump at a flow rate of 10 µL/min. Each full MS spectrum was an average of 100 individual scans.

In separate experiments, to promote the deprotonation of **II**b (Figures 1A, S7 and Table 1), 100 µL 1 mM ligand **1**, 100/200/600 µL 1 mM $CuSO_4$, 100 µL 10 mM Na ascorbate, 100 µL 5 mM NaOH, and 600/500/100 µL deoxygenated water were mixed in 3 separate Eppendorf tubes and the spectra were recorded using the above procedure.

To study the solution equilibria of CuAAC reaction (Figure 1B), 100 µL 1 mM ligand **1**, 100/200/300 µL 1 mM $CuSO_4$, 100 µL 1 mM azido-tetraethylene glycol (N_3EG_4), 100 µL 10 mM Na ascorbate, and 600/500/400 µL deoxygenated water, were mixed in 3 separate Eppendorf tubes in anaerobic chamber, vortexed, and then immediately infused into ESI source by a syringe pump at a flow rate of 10 µL/min. Reaction time was recorded on a timer. Each full MS spectrum in Figure 1B was an average of scans during the reaction time of 4–6 min. The reaction mixture was continuously infused into the ESI source during a period of 20 min. At Cu/**1** = 3:1, the variation of ESI-MS intensities of selected intermediates during the reaction was plotted on Figure 2A.

Kinetic studies for reaction between 1 and N_3EG_4 (Figure 2B)

The reactions were conducted in an anaerobic chamber at room temperature. Solutions in 900 µL deoxygenated Milli-Q water was added into separate Eppendorf tubes, containing 100 nmol **1**, 1 µmol sodium ascorbate, and: A: 100 nmol $CuSO_4$, B: 200 nmol $CuSO_4$, C: 300 nmol $CuSO_4$, D: 100 nmol $CuSO_4$ and 500 nmol NaOH, E: 200 nmol $CuSO_4$ and 500 nmol NaOH, F: 600

nmol $CuSO_4$ and 500 nmol NaOH. 100 µL 1 mM azido tetraethylene glycol (N_3EG_4) aqueous solution was added into each tube to initiate the reaction. At 20 s (for A, B, C) or 10 s (for D, E, F) intervals, 20 µL aliquots of the reaction mixture were added into a 96-well plate, each well containing 180 µL air-saturated aqueous solution of 20 nmol diethylene triamine pentaacetic acid (DTPA) (pH adjusted to 7 by NaOH) as the quenching reagent and 1 nmol **5** (structure shown in Scheme S1) as internal standard. After 8 aliquots were collected, the 96-well plate was moved out of anaerobic chamber. The samples were injected to a Thermo Finnigan LCQ Deca XP Plus ion trap mass spectrometer through a Thermo Finnigan Surveyor HPLC system. Reagents and product were separated by first static elution in 3% (MeCN, 0.1% formic acid) : 97% (H_2O, 0.1% formic acid) for 5 min and then a linear gradient elution to 95% (MeCN, 0.1% formic acid) : 5% (H_2O, 0.1% formic acid) for 5 min. A set of calibration standards of product **2**, ranging from 100 nM to 10 µM, using **5** as internal standard, was injected before the unknowns. The concentration of product **2** in each sample was calculated based on the calibration curve. Each reaction under same condition was repeated three times.

ESI-MS analysis for intermediate solution equilibria in Cu^{I}_{n}3 solutions (Figure 3B, S17)

ESI-MS spectra of Cu^{I}_{n}**3** solutions were acquired using a Thermo Finnigan LCQ Deca XP Plus ion trap mass spectrometer at capillary temperature of 40°C, spray voltage 4.5 kV, capillary voltage 32 V, multipole 1 offset 5V, multipole 2 offset 12V, entrance lens voltage 51 V. In an anaerobic chamber, all stock solutions were prepared in deoxygenated Milli-Q water.

To study the solution equilibria of **3**/Cu = 10:6 solution (Figure 3B), 50 µL of 10 mM sodium ascorbate was added into 950 µL of aqueous solution containing 100 nmol **3**, 60 nmol $CuSO_4$, and 60/30/20 nmol **TL**.

To study the solution equilibria of **3**/Cu = 100:6 solution (Figure S17), 50 µL of 10 mM sodium ascorbate was added into 950 µL of aqueous solution containing 1 µmol **3**, 60 nmol $CuSO_4$, and 120/60/30/20/15/0 nmol **TL**.

The mixtures were directly infused into ESI source by a syringe pump at a flow rate of 10 µL/min. Each full MS spectrum was an average of about 100 individual scans. Zoom scan analysis was carried out to determine the charge state and isotopic pattern for selected Cu^{I} adducts. Each zoom scan spectra represents an average of 50**–**100 individual scans (Figure S18). MS/MS analysis were carried out to determine the fragmentation pattern of selected Cu^{I} adducts (Figure S19).

Rate order studies for reaction between 3 and N_3EG_4 with various amount of Cu^{I} (Figure 3C)

In an anaerobic chamber, eight 1 mL Titertube® micro test tubes (Bio-Rad) were placed in a 96-well Titertube rack. Solutions in 900 µL deoxygenated Milli-Q water (pH=7.0) was added into these tubes, each containing 100 nmol **3**, 100 nmol azido tetraethylene glycol and 10, 20, 30, 40, 60, 80, 100 nmol [$(CuSO_4)_3$(**TL**)] or [$(CuSO_4)_2$(**TL**)] or [$(CuSO_4)$(**TL**)]. 100 µL of 5 mM sodium ascorbate aqueous solution was added into each tube simultaneously by a multichannel pipette to start the reaction. At 1 min intervals, 100 µL aliquots of the reaction mixture were added into a 96-well plate, each well containing 90 µL air-saturated diethylene triamine pentaacetic acid (DTPA) aqueous solution (pH adjusted to 7.0 by NaOH). After 6 sets of aliquots were collected, the 96-well plate was moved out of anaerobic chamber. 10 µL 100 µM **S10** (structure shown in Scheme S1) water solution was added into each aliquot as internal standard. The samples were injected to a Thermo Finnigan LCQ Deca XP Plus ion trap mass spectrometer through a Thermo Finnigan Surveyor HPLC system. Reagents and product were separated by first static elution in 3% (MeCN, 0.1% formic acid) : 97% (H_2O, 0.1% formic acid) for 2 min and then a linear gradient elution to 90% (MeCN, 0.1% formic acid) : 10% (H_2O, 0.1% formic acid) for 5 min. A set of calibration standards of product **4**, ranging from 500 nM to 50 µM, using **S10** as internal standard, were injected before and after each set of samples. The concentration of product in each sample was calculated based on the calibration curve.

Acknowledgements

This work was supported by the National Institute of Health grant (5R01EY013175), the National Science Foundation grant (DMR-1508722), and the GEAR grant from the University of Houston. We thank Dr. R. Thummel, Dr. S. Bark and Dr. M. Hu for permission and help to use their equipment.

Keywords: Click Chemistry • CuAAC Reaction • Reactive Intermediate • Mass Spectrometry • Tri-copper Acetylide

[1] a) V. V. Rostovtsev, L. G. Green, V. V. Fokin and K. B. Sharpless, *Angew. Chem.* **2002**, *114*, 2708 2711; *Angew. Chem., Int. Ed.* **2002**, *41*, 2596 2599; b) C. W. Tornøe, C. Christensen and M. Meldal, *J. Org. Chem.* **2002**, *67*, 3057 3064.

[2] a) M. Meldal and C. W. Tornøe, *Chem. Rev.* **2008**, *108*, 2952 3015; b) P. L. Golas and K. Matyjaszewski, *Chem. Soc. Rev.* **2010**, *39*, 1338 1354; c) E. Lallana, R. Riguera and E. Fernandez-Megia, *Angew. Chem.* **2011**, *123*, 8956 8966; *Angew. Chem., Int. Ed.* **2011**, *50*, 8794 8804; d) P. Thirumurugan, D. Matosiuk and K. Jozwiak, *Chem. Rev.* **2013**, *113*, 4905 4979; e) Craig S. McKay and M. G. Finn, *Chem. Biol.* **2014**, *21*, 1075 1101.

[3] a) V. O. Rodionov, V. V. Fokin and M. G. Finn, *Angew. Chem.* **2005**, *117*, 2250 2255; *Angew. Chem., Int. Ed.* **2005**, *44*, 2210 2215; b) R. Berg and B. F. Straub, *Beilstein J. Org. Chem.* **2013**, *9*, 2715 2750; c) M. Ahlquist and V. V. Fokin, *Organometallics* **2007**, *26*, 4389 4391; d) B. F. Straub, *Chem. Commun.* **2007**, 3868 3870; e) D. Cantillo, M. Avalos, R. Babiano, P. Cintas, J. L. Jimenez and J. C. Palacios, *Org. Biomol. Chem.* **2011**, *9*, 2952 2958; f) I. Kalvet, J. Tammiku-Taul, U. Mäeorg, K. Tämm, P. Burk and L. Sikk, *ChemCatChem* **2016**, *8*, 1804 1808; g) L. Zhu, C. J. Brassard, X. Zhang, P. M. Guha and R. J. Clark, *Chem. Rec.* **2016**, *16*, 1501 1517; h) G.-C. Kuang, P. M. Guha, W. S. Brotherton, J. T. Simmons, L. A. Stankee, B. T. Nguyen, R. J. Clark and L. Zhu, *J. Am. Chem. Soc.* **2011**, *133*, 13984 14001.

[4] S. S. Y. Chui, M. F. Y. Ng and C.-M. Che, *Chem. Eur. J.* **2005**, *11*, 1739 1749.

[5] a) C. Nolte, P. Mayer and B. F. Straub, *Angew. Chem.* **2007**, *119*, 2147 2149; *Angew. Chem., Int. Ed.* **2007**, *46*, 2101 2103; b) B. T. Worrell, J. A. Malik and V. V. Fokin, *Science* **2013**, *340*, 457 460; c) S. Díez-González and S. P. Nolan, *Angew. Chem.* **2008**, *120*, 9013 9016; *Angew. Chem., Int. Ed*. **2008**, *47*, 8881 8884.

[6] L. Jin, D. R. Tolentino, M. Melaimi and G. Bertrand, *Sci. Adv*. **2015**, *1*.

[7] C. Iacobucci, S. Reale, J.-F. Gal and F. De Angelis, *Angew. Chem.* **2015**, *127*, 3108 3111; *Angew. Chem., Int. Ed.* **2015**, *54*, 3065 3068.

[8] A. Makarem, R. Berg, F. Rominger and B. F. Straub, *Angew. Chem.* **2015**, *127*, 7539 7543; *Angew. Chem., Int. Ed.* **2015**, *54*, 7431 7435.

[9] a) C. Hinderling, C. Adlhart and P. Chen, *Angew. Chem.* **1998**, *110*, 2831 2835; *Angew. Chem., Int. Ed.* **1998**, *37*, 2685 2689; b) A. Teichert and A. Pfaltz, *Angew. Chem.* **2008**, *120*, 3408 3410; *Angew. Chem., Int. Ed.* **2008**, *47*, 3360 3362; c) V. Carrasco-Sanchez, M. Simirgiotis and L. Santos, *Molecules* **2009**, *14*, 3989 4021; d) K. L. Vikse, Z. Ahmadi, C. C. Manning, D. A. Harrington and J. S. McIndoe, *Angew. Chem.* **2011**, *123*, 8454 8456; *Angew. Chem., Int. Ed.* **2011**, *50*, 8304 8306; e) A. Tsybizova and J. Roithová, *Mass Spectrom. Rev.* **2016**, *35*, 85 110; f) C. Iacobucci, S. Reale and F. De Angelis, *Angew. Chem.* **2016**, *128*, 3032 3045; *Angew. Chem., Int. Ed.* **2016**, *55*, 2980 2993; g) S. Banerjee, C. Basheer and R. N. Zare, *Angew. Chem.* **2016**, *128*, 12999 13003; *Angew. Chem., Int. Ed.* **2016**, *55*, 12807 12811.

[10] a) T. R. Chan, R. Hilgraf, K. B. Sharpless and V. V. Fokin, *Org. Lett.* **2004**, *6*, 2853 2855; b) V. Hong, S. I. Presolski, C. Ma and M. G. Finn, *Angew. Chem.* **2009**, *121*, 10063 10067; *Angew. Chem., Int. Ed.* **2009**, *48*, 9879 9883; c) V. Hong, N. F. Steinmetz, M. Manchester and M. G. Finn, *Bioconjugate Chem.* **2010**, *21*, 1912 1916; d) D. Soriano del Amo, W. Wang, H. Jiang, C. Besanceney, A. C. Yan, M. Levy, Y. Liu, F. L. Marlow and P. Wu, *J. Am. Chem. Soc.* **2010**, *132*, 16893 16899; e) C. Besanceney-Webler, H. Jiang, T. Zheng, L. Feng, D. Soriano del Amo, W. Wang, L. M. Klivansky, F. L. Marlow, Y. Liu and P. Wu, *Angew. Chem.* **2011**, *123*, 8201 8206; *Angew. Chem., Int. Ed.* **2011**, *50*, 8051 8056; f) C. Uttamapinant, A. Tangpeerachaikul, S. Grecian, S. Clarke, U. Singh, P. Slade, K. R. Gee and A. Y. Ting, *Angew. Chem.* **2012**, *124*, 5954 5958; *Angew. Chem., Int. Ed.* **2012**, *51*, 5852 5856; g) M. Yang, A. S. Jalloh, W. Wei, J. Zhao, P. Wu and P. R. Chen, *Nat. Commun.* **2014**, *5*, 4891.

[11] a) M. Yang, J. Li and P. R. Chen, *Chem. Soc. Rev.* **2014**, *43*, 6511 6526; b) S. Li, L. Wang, F. Yu, Z. Zhu, D. Shobaki, H. Chen, M. Wang, J. Wang, G. Qin, U. J. Erasquin, L. Ren, Y. Wang and C. Cai, *Chem. Sci.* **2017**, DOI: 10.1039/C6SC02297A.

[12] a) V. O. Rodionov, S. I. Presolski, D. Díaz Díaz, V. V. Fokin and M. G. Finn, *J. Am. Chem. Soc.* **2007**, *129*, 12705 12712; b) S. I. Presolski, V. Hong, S.-H. Cho and M. G. Finn, *J. Am. Chem. Soc.* **2010**, *132*, 14570 14576.

[13] For the crystal structure of a **TL**-Cu^{I}_{3}-acetylide analogue, see CCDC # 1516039. For examples of other multinuclear Cu^{I}_{n}-acetylides containing 3-center-2-electron bonds, see ref. [3h] and [8].

[14] Y. Özkılıç and N. Ş. Tüzün, *Organometallics* **2016**, *35*, 2589 2599.

[15] M. Rae and M. N. Berberan-Santos, *J. Chem. Educ.* **2004**, *81*, 436.

[16] a) Z. Yuan, G.-C. Kuang, R. J. Clark and L. Zhu, *Org. Lett.* **2012**, *14*, 2590 2593; b) V. Bevilacqua, M. King, M. Chaumontet, M. Nothisen, S. Gabillet, D. Buisson, C. Puente, A. Wagner and F. Taran, *Angew. Chem.* **2014**, *126*, 5982 5986; *Angew. Chem., Int. Ed.* **2014**, *53*, 5872 5876.

10.1002/chem.201700555

WILEY-VCH

Entry for the Table of Contents (Please choose one layout)

Layout 1:

FULL PAPER

Tri-Cu acetylides and triazolides in CuAAC: Mechanistic study of the tris(triazolylmethyl)amine ligand accelerated CuAAC reaction was performed in aqueous solutions. Reactive tri-Cu and di-Cu intermediates were identified by ESI-MS and their CuAAC activity were quantitatively measured by LC-MS.

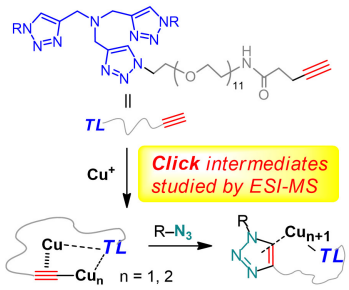

Haoqing Chen, Chengzhi Cai, Siheng Li, Yong Ma, Sijin Luozhong, Zhiling Zhu*

Page No. – Page No.

Intermediates Stabilized by Tris(triazolylmethyl)amines in CuAAC Reaction